

A New Measurement of $\eta_b(1S)$ From $\Upsilon(3S)$ Radiative Decay at CLEO

Sean Dobbs (for the CLEO Collaboration)

Northwestern University, Evanston, IL 60208, USA

Abstract. Using CLEO data, we report on the confirmation of the $\eta_b(1S_0)$ ground state of bottomonium in the radiative decay $\Upsilon(3S) \rightarrow \gamma\eta_b$. We determine its mass to be $M(\eta_b) = 9391.8 \pm 6.6 \pm 2.1$ MeV, which corresponds to the hyperfine splitting $\Delta M_{hf}(1S) = 68.5 \pm 6.6 \pm 2.0$ MeV, and the branching fraction $\mathcal{B}(\Upsilon(3S) \rightarrow \gamma\eta_b) = (7.1 \pm 1.8 \pm 1.1) \times 10^{-4}$. These results agree with those previously reported by BaBar.

Keywords: Bottomonium Spectroscopy, Upsilon, Quarkonia

PACS: 14.40.Pq, 12.38.Qk, 13.25.Gv

INTRODUCTION

Bottomonium ($|b\bar{b}\rangle$) is the preferred system for the study of the $q\bar{q}$ interaction. Theoretical calculations for bottomonium are generally more reliable than for other $q\bar{q}$ systems due to the small relativistic corrections ($v/c \approx 0.1$). However, much about the spectrum of bottomonium states remains unknown. Although potential models predict ~ 26 bottomonium states to lie below the $B\bar{B}$ threshold (as illustrated in Fig. 1), only 10 of them had been identified since the discovery of bottomonium in 1977 [1] until 2008. Most importantly, the ground state $\eta_b(1S_0)$, had not been identified, despite many searches by CUSB [2] and CLEO [3] at CESR, and ALPEH [4] and DELPHI [5] at LEP, among others.

This situation changed in July 2008, when the BaBar Collaboration announced the discovery of $\eta_b(1S)$ in their data for 109 million $\Upsilon(3S)$ [6, 7] in the radiative decay $\Upsilon(3S) \rightarrow \gamma\eta_b(1S)$, with a significance of $> 10\sigma$, as illustrated in Fig. 2. We note that the small peak at $E_\gamma \approx 920$ MeV due to the radiative transition to $\eta_b(1S)$ is not visible until the large smooth background is subtracted. BaBar's success is due not simply due to their large data set, more than an order of magnitude larger than previously collected at CLEO, but also due a factor 3 greater background suppression by the use of a cut on the ‘‘thrust angle’’. The thrust angle is defined as the angle between the signal transition photon candidate and the thrust axis of the rest of the event [8].

BaBar's discovery of η_b is exciting and like all such claims, needs to be confirmed by an independent experiment. We report on such a measurement at CLEO.

ANALYSIS OF CLEO DATA

At CLEO we have an 18 times smaller data set than BaBar (5.9M compared to 109M), so several improvements in analysis procedure were needed in order to identify the η_b signal. The three main improvements were: performing a detailed study of the background parameterization; obtaining accurate parameterizations of the photon peak line shapes; and using the power of the thrust angle to separate signal and background to perform a joint analysis of the full data in three bins of the thrust angle.

In Fig. 2, we show the inclusive energy spectra for isolated electromagnetic showers in CLEO $\Upsilon(3S)$ and $\Upsilon(2S)$ data, after contributions from $\pi^0 \rightarrow \gamma\gamma$ have been rejected. Three features are immediately visible from these spectra. One, the spectra are dominated by a larger, smoothly varying background from other bottomonium decays and decays from $e^+e^- \rightarrow \gamma^* \rightarrow$ lighter hadrons. Two, the visible peaks come from the unresolved transitions $\chi_{bJ}(2P, 1P) \rightarrow \gamma\Upsilon(1S)$, $J = 0, 1, 2$. Lastly, the peaks from $e^+e^- \rightarrow \chi_{SR}\Upsilon(1S)$ and $\Upsilon(3S, 2S) \rightarrow \gamma\eta_b(1S)$ (with $E_\gamma(\eta_b) \approx 600$ MeV for $\Upsilon(2S)$ and $E_\gamma(\eta_b) \approx 920$ MeV for $\Upsilon(3S)$) are expected to be more than an order of magnitude weaker than the $\chi_{bJ}(2P, 1P)$ peaks, and they reside on the high energy tails of $\chi_{bJ}(2P, 1P)$.

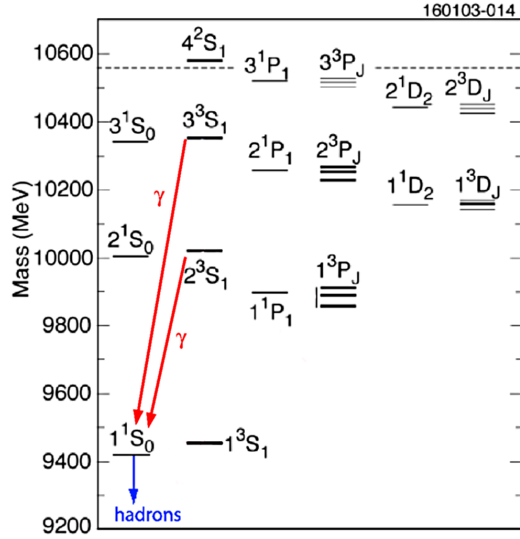


FIGURE 1. Spectrum of the bound bottomonium ($b\bar{b}$) states. The M1 transitions from the $\Upsilon(n^3S_1)$ states to the $\eta_b(1^1S_0)$ are indicated by red arrows for the transitions reported in this paper.

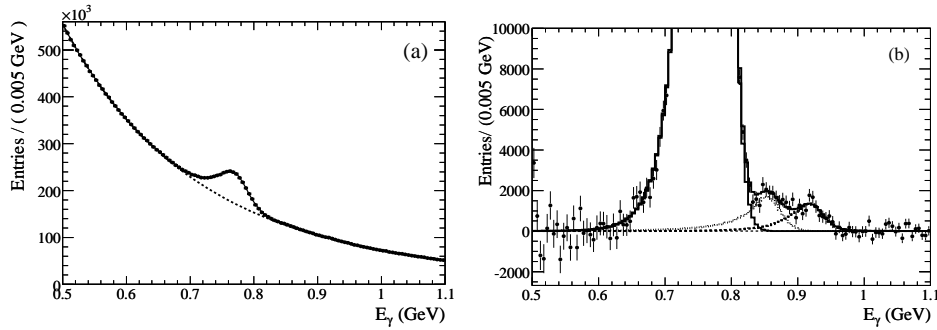


FIGURE 2. BaBar results for the observation of η_b [6]. (Left) The observed inclusive photon spectrum. (Right) The background subtracted photon spectrum. The peaks, from left to right, are from χ_{bJ} , $\Upsilon(1S)$ ISR, and η_b .

Photon Line Shapes: Photon line shapes in crystal calorimeters, like those used by CLEO, are generally parameterized in terms of the Crystal Ball function. This function combines a Gaussian (width σ), with a low-energy power law tail (parameters α and n). Knowing the shape of the low energy tail is especially important for the χ_{bJ} peaks, since they are important in determining the shape of the background at the energy of the small η_b signal. These parameters must be determined by fitting a background-free photon peak. In our analysis we use two independent methods. In one method, we use the observed shape of photons from a given energy from radiative Bhabha events, and in the other we use the shape of photons from the exclusive decays $\chi_{b1}(2P, 1P) \rightarrow \gamma\Upsilon(1S)$, $\Upsilon(1S) \rightarrow l^+l^-$. Both methods give consistent results, and once the parameters are determined, they are fixed in subsequent analyses.

ISR Peak: All the parameters of the ISR photon peak from $\Upsilon(nS) \rightarrow \gamma_{\text{ISR}}\Upsilon(1S)$ were fixed. The yield of the ISR peak was estimated by extrapolating the observed yield in CLEO data taken at $\Upsilon(4S)$, and was then fixed to this value.

Background: We find that fitting the smooth background is the most crucial component in determining the results for the weak η_b peak. We made several hundred background fits to the data in each of three bins of $|\cos\theta_T|$, using exponential polynomials of various orders (2,3,4), in various energy regions (500–1340 MeV), and with linear and logarithmic binning of the data. We found that many of these fit the data acceptably, and took as our final results the average of $E_\gamma(\eta_b)$, $\mathcal{B}(\Upsilon(nS) \rightarrow \gamma\eta_b)$, and significance for all the good fits (CL > 10%). The r.m.s. variation of these fits was then taken as a measure of the systematic uncertainty in the results from this source, ± 1 MeV in E_γ , $\pm 10\%$ in $\mathcal{B}(\eta_b)$, and $\pm 0.4\sigma$ in significance.

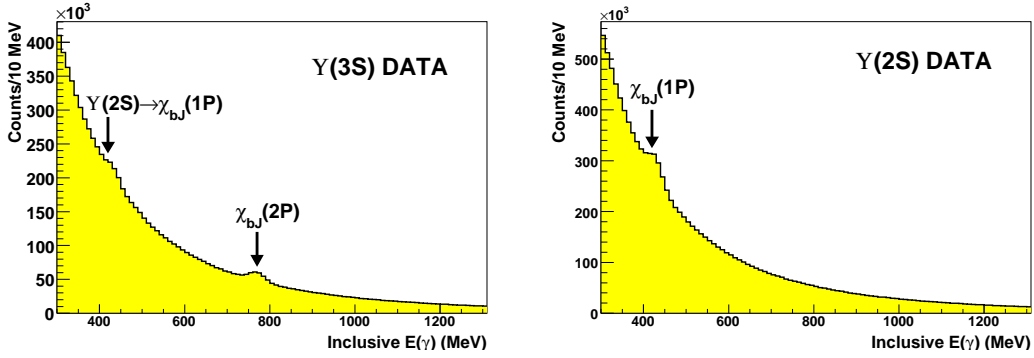


FIGURE 3. CLEO inclusive photon spectra for (left) $Y(3S)$ decay, and (right) $Y(2S)$, illustrating the broad features described in the text.

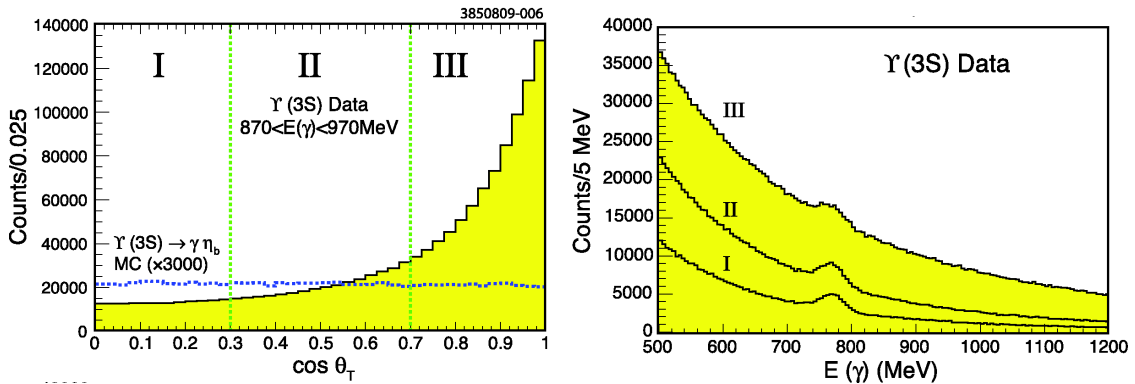


FIGURE 4. (Left) Thrust angle $|\cos \theta_T|$ distribution for $Y(3S)$ data in the expected η_b signal region, and the expected distribution for the η_b signal from MC simulations. (Right) Inclusive photon spectra for the data in the three thrust angle regions, illustrating their different signal/background ratios.

Joint Analysis in Three Bins of $|\cos \theta_T|$: As Fig. 4 (left) shows, the distribution of thrust angle ($|\cos \theta_T|$) for the background-dominated data is strongly peaked in the forward direction, but for the transition photon to the η_b , the distribution is expected to be uniform. This happens because the transition photon is uncorrelated with the particles produced by the decay of the η_b , whereas the background photons tend to be correlated with the other particles produced in the underlying event. We therefore define three different regions of $|\cos \theta_T|$: region I ($|\cos \theta_T| = 0 - 0.3$), region II ($|\cos \theta_T| = 0.3 - 0.7$), and region III ($|\cos \theta_T| = 0.7 - 1.0$). Fig. 4 (right) illustrates the different levels of signal and background in the three regions.

Unlike BaBar, we do not reject events in the $|\cos \theta_T| > 0.7$ region. Instead, we simultaneously fit the spectra for each of the three regions, which lets each region contribute to the total result weighted by its individual signal-to-background. We call this method the “joint fit”. We have analyzed our data by the joint fit method, and also with $|\cos \theta_T| < 0.7$, for comparison with BaBar’s method. We find that the joint fit method enhances the significance of the η_b identification by $\sim 1\sigma$.

JOINT FIT RESULTS

We show a representative fit for the three bins of thrust angle in Fig. 5. The results of the fit are: $N(\eta_b) = 2311 \pm 546$ counts, $E_\gamma(\eta_b) = 918.6 \pm 6.0(\text{stat})$ MeV, which corresponds to the hyperfine splitting of 68.5 ± 6.6 MeV, $\mathcal{B}(Y(3S) \rightarrow \gamma\eta_b) = (7.1 \pm 1.8(\text{stat})) \times 10^{-4}$, and significance 4.1σ .

Although we fix $\Gamma(\eta_b) = 10$ MeV, because the width of η_b is unknown we find that the branching fraction depends on the assumed η_b width linearly as $\mathcal{B}(Y(3S) \rightarrow \gamma\eta_b) \times 10^4 = 5.8 + 0.13(\Gamma(\eta_b) \text{ in MeV})$. Our results are dominated

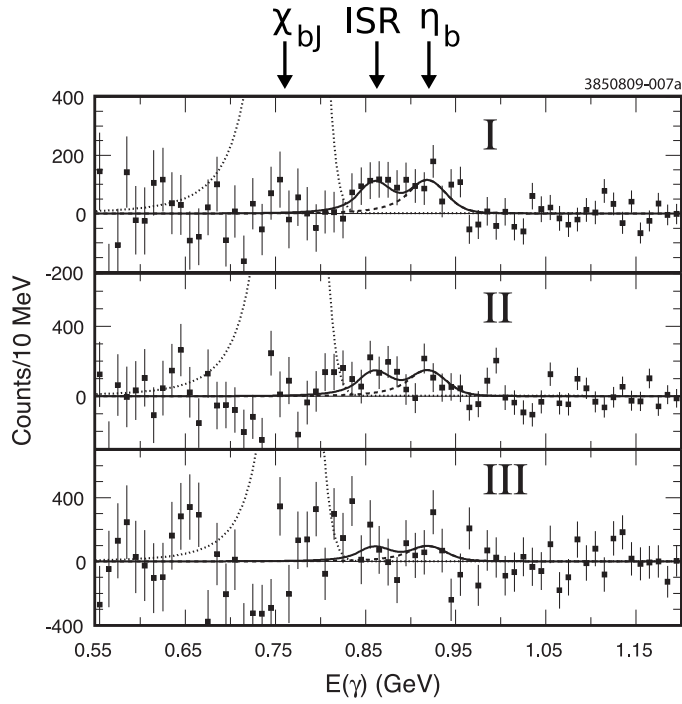


FIGURE 5. Background subtracted spectra and representative fit result for $\Upsilon(3S) \rightarrow \gamma\eta_b(1S)$. The $\eta_b(1S)$ peak is clearly visible in $|\cos\theta_T|$ region I and II.

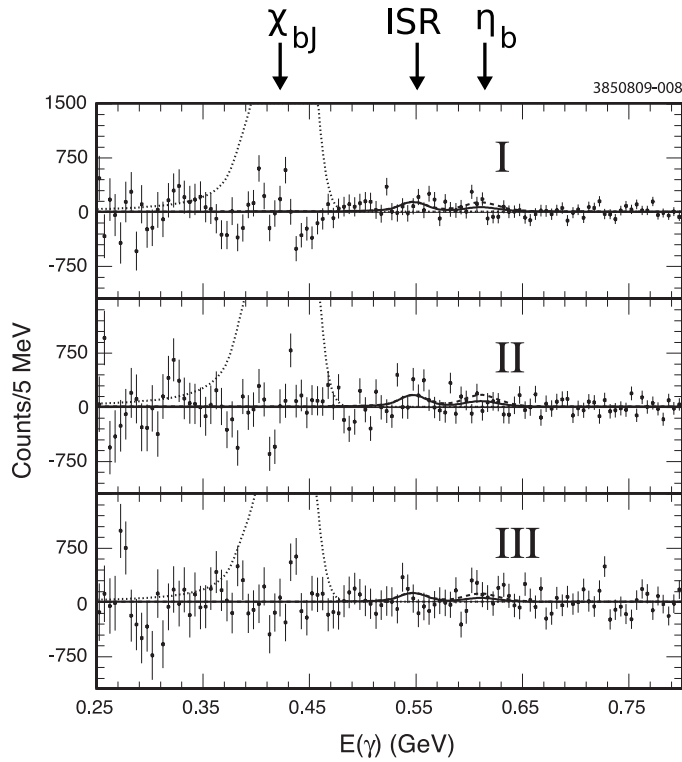


FIGURE 6. Background subtracted spectra and representative fit result for $\Upsilon(2S) \rightarrow \gamma\eta_b(1S)$. The dashed line corresponds to the 90% CL upper limit given in the text. The $\eta_b(1S)$ is not seen in any of the three regions of $|\cos\theta_T|$.

TABLE 1. Systematic uncertainties in measurement of $\Upsilon(3S) \rightarrow \gamma\eta_b$ photon energy and branching fractions.

Source	Uncertainty in	
	E_γ (MeV)	$\mathcal{B}(\Upsilon(3S) \rightarrow \gamma\eta_b)$
Background (fn, range, binning)	± 1.0	$\pm 10\%$
Photon Energy Calibration	± 1.2	—
Photon Energy Resolution	± 0.3	$\pm 2\%$
CB and $\chi_{bj}(2P)$ Parameters	± 0.7	$\pm 8\%$
ISR Yield	± 0.4	$\pm 3\%$
Photon Reconstruction	—	$\pm 2\%$
$N(\Upsilon(3S))$	—	$\pm 2\%$
MC Efficiency	—	$\pm 7\%$
Total	± 1.8	$\pm 15\%$

TABLE 2. Summary of η_b results from CLEO and BaBar for hyperfine splitting $\Delta M_{hf}(1S)_{b\bar{b}}$ and branching ratio, and comparison with theoretical predictions.

		$\Delta M_{hf}(1S)_{b\bar{b}}$, (MeV)	$\mathcal{B}(\Upsilon(nS) \rightarrow \gamma\eta_b) \times 10^4$	significance
$\Upsilon(3S) \rightarrow \gamma\eta_b$	(CLEO) [9]	$68.5 \pm 6.6 \pm 2.0$	$7.1 \pm 1.8 \pm 1.1$	4σ
	(BaBar) [6]	$71.4^{+3.1}_{-2.3} \pm 2.7$	$4.8 \pm 0.5 \pm 0.6$	$\geq 10\sigma$
$\Upsilon(2S) \rightarrow \gamma\eta_b$	(CLEO) [9]	—	< 8.4 (90% CL)	—
	(BaBar) [7]	$66.1^{+4.9}_{-4.8} \pm 2.0$	$3.9 \pm 1.1^{+1.1}_{-0.9}$	3.0σ
Lattice (UKQCD+HPQCD) [10]	(TWQCD) [11]	61 ± 14		
	(Ehrman) [12]	70 ± 5		
		37 ± 8		
pQCD (various)		$35 - 100$	$0.05 - 25$ ($\Upsilon(3S)$)	
			$0.05 - 15$ ($\Upsilon(2S)$)	

by their statistical uncertainties; the systematic uncertainties were determined conservatively and are given in Table 1. We further note that although we quote an uncertainty in photon energy calibration of ± 1.2 MeV, the energies of the ISR peak and the $\chi_{bj}(2P)$ centroid agree with their expected energies within ± 0.3 MeV.

The analysis method described for $\Upsilon(3S)$ was also used for our $\Upsilon(2S)$ data. Because the background near the expected $\Upsilon(2S) \rightarrow \gamma\eta_b(1S)$ signal ($E_\gamma \approx 610$ MeV) is approximately 6 times higher than the corresponding $\Upsilon(3S)$ (see Fig. 3) transition, no evidence for the excitation of η_b was observed in any $|\cos\theta_T|$ bin, as illustrated in Fig. 6. The joint analysis led to an upper limit of $\mathcal{B}(\Upsilon(2S) \rightarrow \gamma\eta_b) < 8.4 \times 10^{-4}$, at 90% confidence level.

We summarize our results and compare them to BaBar’s results in Table 2. Both results are in agreement. In Table 2 we also list the theoretical predictions for hyperfine splitting and branching ratio. The various potential model predictions vary over a wide range. Lattice calculations for the hyperfine splitting are also given [10, 11, 12], which generally agree with the experimental results.

REFERENCES

1. S. W. Herb *et al.*, *Phys. Rev. Lett.* **39**, 252 (1977).
2. P. Franzini *et al.*, (CUSB Collaboration), *Phys. Rev.* **D 35**, 2883 (1987).
3. M. Artuso *et al.* (CLEO Collaboration), *Phys. Rev. Lett.* **94**, 032001 (2005).
4. A. Heister *et al.* (ALEPH Collaboration), *Phys. Lett.* **B 530**, 56 (2002).
5. J. Abdallah *et al.* (DELPHI Collaboration), *Phys. Lett.* **B 634**, 340 (2006).
6. B. Aubert *et al.* (BABAR Collaboration), *Phys. Rev. Lett.* **101**, 071801 (2008).
7. B. Aubert *et al.* (BABAR Collaboration), *Phys. Rev. Lett.* **103**, 161801 (2009).
8. S. Brandt *et al.*, *Phys. Lett.* **12**, 57 (1964); E. Farhi, *Phys. Rev. Lett.* **39**, 1587 (1977).
9. G. Bonvicini *et al.* (CLEO Collaboration), submitted to *Phys. Rev. Lett.* [arXiv:0909.5474].
10. A. Gray *et al.*, (HPQCD and UKQCD Collaborations), *Phys. Rev.* **D 72**, 094507 (2005).
11. T. Burch and C. Ehmann, *Nucl. Phys.* **A 797**, 33 (2007).
12. T. W. Chiu, T. H. Hsieh, C. H. Huang and K. Ogawa (TWQCD Collaboration), *Phys. Lett.* **651**, 171 (2007).